Kinetic stability of complex molecular clusters

Sukina Natarajan[a)]
Department of Physics and Astronomy, University College London, Gower Street, London WCIE 6BT, United Kingdom

Sarah A. Harris
Department of Physics and Astronomy, University College London, Gower Street, London WCIE 6BT, United Kingdom and School of Physics and Astronomy, University of Leeds, Leeds LS2 9JT, United Kingdom

Ian J. Ford
Department of Physics and Astronomy, University College London, Gower Street, London WCIE 6BT, United Kingdom

(Received 28 October 2005; accepted 1 December 2005; published online 30 January 2006)

This investigation is concerned with modeling the evaporation, or decay, of *n*-nonane molecular clusters. We use a unique cluster decay model that was first developed to estimate the decay time scale of argon clusters using molecular-dynamics simulations. In this study we seek to enhance the model so that it represents a more complex cluster decay dynamic, suitable for *n*-nonane clusters. Experimental measurements of nucleation rates of *n*-nonane droplets have been used to deduce the rate at which a molecule escapes from the cluster. Typically for an *n*-nonane cluster containing 40 molecules, at an experimental temperature of 225 K, the empirical decay time, which is the inverse of the decay rate, is estimated to be 50 ns. For this time scale, the direct observation of *n*-nonane cluster decay from a molecular-dynamics trajectory is not feasible, since decay events are so rare. However, the cluster decay model uses a combination of molecular dynamics and stochastic dynamics in order to resolve the problem associated with long decay time scales. The model is based on a Langevin treatment that views cluster decay as single-particle escape from a confining potential of mean force. It is used to predict kinetic decay times of *n*-nonane clusters. We discover this result differs significantly from a classically derived decay time scale determined from a continuum thermodynamic treatment of the population balance equations of clusters. However, the dynamically generated results obtained from the kinetic decay model compare more favorably than the classical results with the empirical decay times that are deduced from experimental measurements of *n*-nonane clusters. © *2006 American Institute of Physics*. [DOI: 10.1063/1.2160511]

I. INTRODUCTION

Under certain conditions, the condensation phase transition of a vapor to a liquid necessitates the nucleation of molecular clusters. The molecular clusters form due to random fluctuations of vapor density. They can either grow by colliding with vapor molecules that stick due to attractive intermolecular interactions, or decay by losing cluster molecules that are moving too fast to be held within the attraction. Once a molecular cluster reaches a certain size, the increase in binding energy due to the condensation starts to balance the unfavorable change in entropy associated with forming a high-density region. This is the critical cluster size, an agglomerate of the new phase with an equal probability of growth or decay. Beyond this stage the cluster can quickly grow into a macroscopic droplet of high density and eventually into the new phase.

We seek to understand the complex dynamical process by which a molecular cluster reaches the critical cluster size, through an investigation into the dynamic stability of molecular clusters. In this work we pursue a theoretical approach to model the cluster decay mechanism of clusters of complex molecules. We employ a dynamic decay model to predict the rate at which molecules escape from the cluster, which we refer to as the kinetic decay rate. The reciprocal of this rate is the mean lifetime of the cluster. The evaporation process is viewed as a collective phenomenon whereby a molecule acquires sufficient kinetic energy to escape the attractive interactions of the cluster, driven by its collisions with the neighboring molecules.

In the next section, we describe how decay rates may be extracted from experimental data, and from the frequently used classical theory of nucleation.

II. CLASSICAL AND EMPIRICAL DECAY RATES

A familiar approach widely used for the treatment of molecular clusters is classical nucleation theory (CNT).[1–3] Originally formulated to provide a measure of stability for droplets, it carries major uncertainties when used to describe microscopic clusters. This is because it treats the molecular cluster as a perfectly spherical droplet of material resembling the bulk liquid, and in doing so uses bulk properties of the liquid-vapor interface to describe the microscopic properties of the molecular cluster. Although this approach is justified for macroscopic droplets, which have a relatively large

[a)]Electronic mail: sukina.natarajan@ucl.ac.uk

surface-to-volume ratio, it is unrealistic for microscopic clusters that can contain just a few molecules. However, at present it remains the most widely accepted formalism for modeling nucleation processes. We follow the usual thermodynamic classical treatment combined with population balance equations of clusters to extract the classical cluster decay rate. One of our aims is to compare this with our dynamically generated kinetic decay rate.

The population dynamics of molecular clusters can be modeled using a set of simple rate equations first proposed by Becker and Döring[2] that describe the cluster's growth and decay. In the steady state, the average number of growth events from an $i-1$ to an i-sized cluster minus the average number of decay events from an i to an $i-1$ sized cluster, per second, is described by the nucleation current J_i. At thermal equilibrium, which corresponds to a saturated vapor ($J_i=0$) we relate the decay rate γ_i to the growth rate β^e_{i-1} of the $(i-1)$ cluster in saturated conditions, and the equilibrium populations n^e_{i-1} and n^e_i, according to

$$\beta^e_{i-1} n^e_{i-1} = \gamma_i n^e_i. \tag{1}$$

In CNT, the populations in thermal equilibrium are related to the surface properties of the clusters, presumed to depend on the surface tension σ of the bulk condensate,[1]

$$n^e_i \propto \exp\left(-\frac{4\pi R_i^2 \sigma}{kT}\right), \tag{2}$$

where R_i is the radius of a spherical droplet, which has a volume equivalent to a cluster containing the same number of molecules. R_i is estimated by Eq. (3),

$$iV_m = \frac{4\pi R_i^2}{3}, \tag{3}$$

where V_m is the volume of a molecule estimated from temperature-dependent bulk density measurements.[4] We assume that the mean rate of monomer attachment can be determined from the kinetic theory of collisions between molecules and a sphere, assuming that all collisions stick. The mean rate of growth of an $i-1$ cluster, in saturated vapor, is then given approximately by Eq. (4),

$$\beta^e_{i-1} = \left(\frac{4\pi R_i^2 kT}{(2\pi mkT)^{1/2}}\right) n^e_1. \tag{4}$$

The term in the brackets is a collision cross section of a sphere, multiplied by a velocity. The mass of the molecule is given by m.

We can use these models to estimate classical cluster decay rates by combining Eqs. (1) and (2) to give

$$\gamma^{\mathrm{CNT}}_i = \beta^e_{i-1} \exp\left(\frac{4\pi(R_i^2 - R_{i-1}^2)\sigma}{kT}\right). \tag{5}$$

However, this classical decay time scale is merely an approximation, particularly for clusters consisting of small numbers of molecules. It is unlikely to compare well with an estimate of the kinetic decay times obtained from empirical knowledge of the systems behavior at the critical cluster size.

Experiments condensing n-nonane vapor in the presence of a carrier gas of helium have been performed at a range of temperatures and supersaturations.[4] From this measurements of the rate of formation of new droplets, otherwise known as the nucleation current, have been used to deduce the critical cluster sizes of n-nonane clusters under the prevailing conditions[5] using the first nucleation theorem.[6] Quantitatively, the measurements show that clusters of size 40, 50, and 67 molecules are critical at temperatures of approximately 225, 250, and 300 K, and at supersaturations of 65, 25, and 6, respectively.[7] Since we expect these clusters to have an equal probability of growth and decay, we can determine their decay rate from Eq. (4), evaluated at the appropriate experimental conditions, explicitly given by Eq. (6),

$$\gamma^{\mathrm{emp}}_i = \left(\frac{4\pi(3mi/4\pi\rho)^{2/3} kT}{(2\pi mkT)^{1/2}}\right) n^e_1. \tag{6}$$

We use the the bulk liquid density ρ together with Eq. (3) to estimate the cluster radius. Although this is not an empirical cluster measurement, it is a reasonable approximation of the average cluster density, which is estimated from direct measurements of the cluster radius using graphics visualization of the molecular dynamics (MD), assuming the cluster has a spherical volume.

This empirical method of calculating the cluster decay times is almost entirely based on experimental measurements of cluster properties rather than measurements of the bulk phase, and thus eliminates the unrealistic approximations made by CNT. Furthermore, all the parameters in Eq. (6) can be reliably estimated from experimental measurements. We expect the calculations based on the empirical properties of the critical cluster sizes to be a good benchmark for comparison with dynamically generated kinetic decay times. This comparison is made in Sec. IV, and in the next section we describe the details of the molecular and stochastic models used to estimate the kinetic decay times.

III. MODEL AND METHODS

A. Small system thermodynamics

MD is a powerful tool that is often used to study microscopic systems. For a system in thermal equilibrium it is essential that there be a suitable means of controlling the temperature. For a small number of molecules, this can be a difficult problem and consequently the issue of small system thermodynamics is often avoided by treating such systems in isolation, which fixes the total energy even though this means the thermodynamic temperature cannot be completely defined. The relation between energy and temperature illustrates the complementarity that exists between these two thermodynamic quantities, which was first proposed by Bohr and Heisenberg,[8] and later characterized further by Uffink and van Dis.[9]

In the case of molecular clusters, however, which would normally interact with a carrier gas under experimental conditions, fixing the cluster's energy is not a realistic approximation.

A molecular cluster that is isolated from its environment does not interact with its surroundings, although its kinetic energy can still vary about a mean. Once this mean has converged, we can characterize the thermal state using the ki-

netic temperature, obtained using the relation $1/2m\langle\nu^2\rangle = 3kT/2$, or by fitting the distribution of velocities to a Maxwell-Boltzmann distribution. We took this approach in an earlier paper.[10] It may be useful to note that the kinetic temperature differs from thermodynamic temperature, which is defined as a derivative of the system entropy $T=\partial E/\partial S$.

However, it would be preferable to impose canonical temperature fluctuations when modeling systems which decay on time scales longer than the thermal equilibration time between the system and its environment. Hence we need to maintain a molecular cluster in thermal contact with a larger system. Fixed temperature dynamics of small systems can be difficult to implement, but it provides a reliable relation between the thermodynamic quantities, energy and temperature. The fluctuations in kinetic energy will be explicitly distributed according to a Maxwell-Boltzmann distribution.

The cluster's kinetic decay rate will be sensitively dependent on the average kinetic energy per molecule since a hot cluster is more likely to decay, and therefore correct thermalization of the cluster is crucial.

To maintain correct thermal equilibrium, the thermostat should populate energetic modes according to the equipartition theorem. For microscopic systems an improper equipartition of energy can lead to problems that would not necessarily be seen in the bulk, such as problems associated with controlling the cluster's angular momentum. A simple yet realistic implementation of the energy exchange between the cluster and carrier gas can be achieved by introducing random energy changes to the cluster atoms, according to the Anderson stochastic thermostat.[11] This approach applied to an isolated cluster mimics the physical effect of the random collisions with molecules in the environment, using random momentum transfers. We assume all cluster atoms are equally likely to suffer a collision, at a given constant probability per unit time. The cluster atom is assigned a new velocity randomly sampled from a Maxwell-Boltzmann distribution at the desired temperature. Analysis of our MD simulations shows that the Anderson thermostat is very effective at controlling the temperature and angular momentum of *n*-nonane clusters subject to random collisions with a carrier gas.

B. Relevant time scales

Under experimental conditions a molecular cluster suffers collisions from the vapor molecules and carrier gas molecules that surround it. Provided there is a sufficiently large number of carrier gas collisions with the cluster on the time scale of vapor collisions with the cluster, it is reasonable to assume that the cluster grows, and by implication decays, when it is at thermal equilibrium with the carrier gas.

We can quantitatively check the relative values of the collision time scales by evaluating typical collision times for the cluster and vapor, and cluster and carrier gas, using Eq. (4). All that needs to be specified is the temperature and supersaturation (the ratio of vapor pressure to saturated vapor pressure), since R_i is determined from the temperature-dependent bulk density, and n_1^e from the supersaturation. The typical collision time between a 40-molecule *n*-nonane cluster and a vapor molecule evaluated at an experimental temperature of 225 K and supersaturation of 65 (i.e., the conditions at which we expect the cluster to be critical), is estimated to be 50 ns. For the helium carrier gas at the typical vapor pressure of 40 kPa (Ref. 4) and the prevailing experimental temperature, the collision time between a carrier gas molecule and the cluster is about 10 ps.

The difference between these time scales is sufficiently large for there to be many carrier gas collisions with the cluster in between vapor collisions with the cluster, and we can therefore assume the cluster to be at thermal equilibrium with the carrier gas. This justifies our treatment of the cluster as a quasistable, fixed temperature system.

In a previous MD study of argon clusters,[12] the mean cluster lifetime was observed to be tens of picoseconds, and during the course of the simulations tens to hundreds of decay events were observed. In the present case of *n*-nonane clusters we have to use a different strategy because the decay time for a typical *n*-nonane cluster is 50 ns. Since decay events are rare, it is difficult to acquire sufficient statistics as it is not feasible to perform MD over such lengthy time scales. We therefore employ a statistical approach to resolve the problems associated with long cluster decay time scales.[12] Our approach is based on a stochastic interpretation of cluster decay, and models the radial motion of a molecule in the cluster using a Langevin equation for noise-driven dissipative motion. We parametrize the Langevin equation by averaging suitable dynamic variables over all cluster configurations within a MD trajectory. This information was used to estimate kinetic decay rates for different cluster sizes of argon, which were in good comparison to directly observed decay rates from MD trajectories.[12]

C. Simulation details

This study is concerned with clusters of complex molecules of *n*-nonane. It is assumed that the escape of these molecules may be described using the earlier treatment of pointlike atoms. *n*-nonane molecules possess an internal structure of bonded interactions, and these additional variables need to be correctly accounted for in order to provide an appropriate description of more a complex decay dynamic. We develop the cluster decay model to predict decay rates of flexible *n*-nonane clusters at a range of experimental temperatures.

The *n*-nonane clusters are treated in isolation from the vapor molecules that are present in their experimental environment. This eliminates the interactions a cluster would normally experience with the surrounding vapor molecules. In this scenario the cluster is not allowed to grow by collision, but it can still lose molecules by evaporation, so decay events can still occur. This treatment significantly increases computational efficiency, yet still retains the key ingredients that are essential to study decay dynamics.

The interactions between atoms of *n*-nonane molecules are described using the GROMOS96 united atom suite of potentials.[13,14] The united atom potential treats the hydrogen atoms implicitly, which is a reasonable approximation since *n*-nonane is overall nonpolar, and the hydrogen atoms have

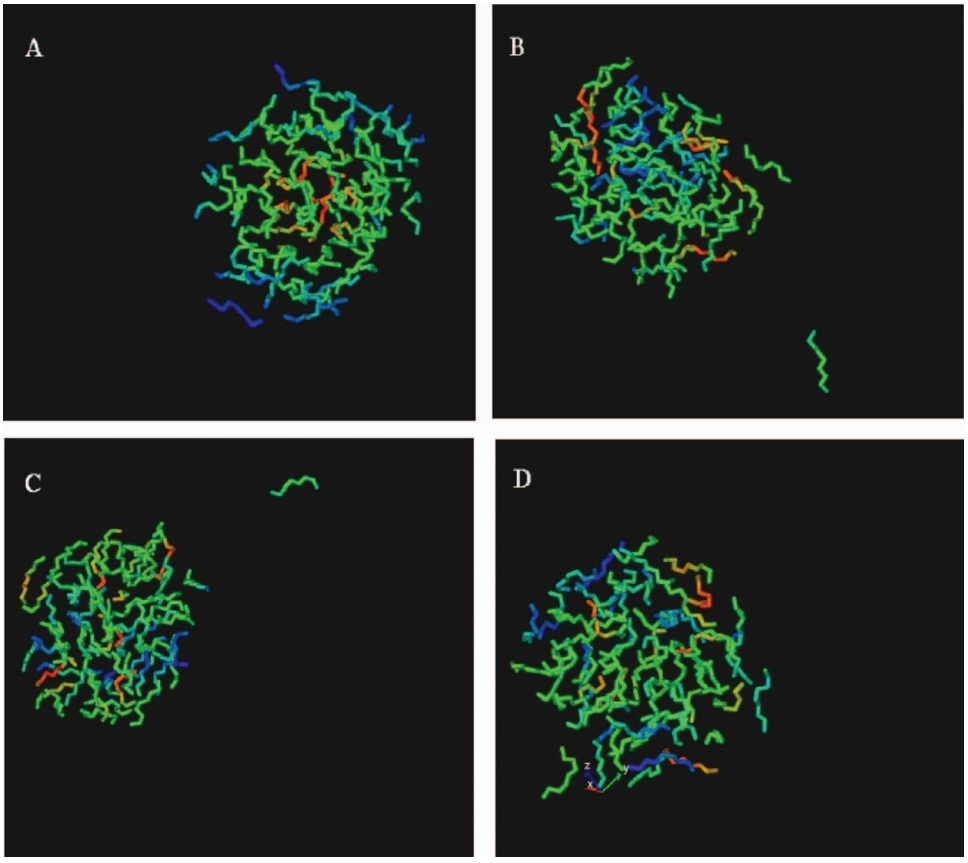

FIG. 1. (Color) A sequence of three-dimensional (3D) molecular-dynamics snapshots of 67 *n*-nonane molecules. The color scheme represents radial position relative to the cluster's center of mass in the first snapshot (A). The second snapshot (B) is taken about 200 ps later, and shows a molecule has escaped. The third snapshot (C) is taken another 200 ps later, just before the molecule recombines with the cluster, and the fourth snapshot (D) is a further 200 ps later, just after it has recombined. An interesting feature of these images is the radial distribution of molecules within the cluster. As we might expect for a liquid cluster, the molecules appear to be disordered, which illustrates the cluster's unstructured fluid nature at 300 K.

little effect on the molecule's overall dynamics. Empirical force fields often fit parameters to experimental data of intermolecular crystal packing or to single molecules in the gas phase.[15] The GROMOS96 force field is directly parametrized to reproduce properties of organic liquids. For this reason it is well suited to describing interactions within organic condensed phase systems, and is assumed in this study to be appropriate for molecular clusters. The potentials comprise of harmonic-bonded interactions as well as Lennard-Jones nonbonded interactions. Each *n*-nonane molecule has a flexible structure, and can undergo translations, rotations, and torsions, as well as vibrations. A molecular-dynamics time step of 0.5 fs is chosen to accommodate the shortest operative mode[16] (vibrational mode). Simulations of *n*-nonane clusters are performed for cluster sizes of 40, 50, and 67 molecules, at the experimental temperatures at which they were deduced to be critical. The simulations are run for approximately 5 ns after equilibration, with a cluster confined to a $10\times10\times10$ nm^3 cubic box with periodic boundary conditions.

During this time the cluster is at thermal equilibrium with the carrier gas. Dynamically, it remains metastable with respect to decay but very occasionally a decay event may be observed. The MD trajectory provides time-evolved center of mass positions, velocities, and forces for all the atoms in the cluster. These quantities are used to parameterize a Langevin treatment of the cluster that is described in the next section.

Figure 1 shows a series of MD snapshots of an *n*-nonane cluster containing 67 molecules, maintained at a temperature of 300 K, generated from the simulations. Clearly there are fewer molecules close to the cluster's center of mass (red) and around the periphery (blue), than within the cluster's main volume (green). This suggests that we might expect the sampling of forces for these regions to be relatively poor due to insufficient statistics.

D. The Langevin treatment of clusters

The approach used by the model views cluster decay as a process of single-particle escape from a constraining potential, driven by a random force due to all the other particles in the cluster (and the carrier gas). Hence, cluster decay is viewed from the perspective of a single molecule in the cluster, and the constraining potential is a potential of mean force. Each molecule in the cluster is considered to move in such a three-dimensional potential well due to its average interactions with all the other cluster molecules that are randomly colliding with it. The radial motion of an individual molecule relative to the cluster's center of mass is modeled using a Langevin equation for noise-driven dissipative motion in a potential well, as shown below,

$$m\ddot{r} = f(r) - m\gamma\dot{r} + \bar{f}(t). \tag{7}$$

The right-hand side of this equation represents the radial force acting on a molecule immersed in a fluid of surrounding particles, as a function of radial position r from the system's center of mass. The first term $f(r)$ is the position-dependent mean force felt by the molecule. This mean force is obtained from the molecular-dynamics trajectory by averaging over all molecular configurations or snapshots for a given radial position of a specified particle. The second term is the velocity-dependent dissipative force acting on the par-

ticle. It is proportional to the friction coefficient γ (not to be confused with the decay rate), and represents the drag experienced by a particle moving through a fluid of surrounding particles. The third term $\tilde{f}(t)$ describes the fluctuations about the mean force brought about by collisions experienced by the particle. It is a random force, independent of velocity and position with a zero mean and a variance related to temperature. We assume the molecular structure has a negligible effect on the dynamics so that the mean interactions act on the molecule's center of mass, and we focus attention on the motion of that center of mass. Whether this approach compromises too much detail of the cluster's decay dynamics is not known, and the significance of this simplification is yet to be clarified.

The equilibrium positional probability distribution $P(r)$ for a particle in a potential of mean force may be shown to take a Boltzmann form.[12] A simple estimate of the kinetic decay rate for a particle in such a potential is therefore proportional to this probability, evaluated at an assumed cluster escape radius r_e. Clearly the depth of the potential of mean force will be a major governing factor for particle escape, and will strongly control the decay time scale. A fuller expression for the kinetic decay rate of a cluster of i molecules is given by Eq. (8) and details of the derivation are given in Ford and Harris,[12]

$$\gamma^{\mathrm{kin}} = \frac{3ir_e kT}{m\gamma R_s^3(1 - R_s/r_e)} \exp\left(-\frac{i\Delta\phi}{(i-1)kT}\right). \tag{8}$$

The particle mass is given by m, and $\Delta\phi_i$ is the depth of the potential of mean force; R_s is an effective radius which is used to model the actual potential of mean force. The cluster escape radius r_e may be estimated for a decay event to be the radius at which the potential of mean force reaches a plateau.

The decay parameters $\Delta\phi$ and γ are determined from the mean force and the frictional force, respectively, which appear in Eq. (7), and are deduced by suitable averaging over all cluster configurations within the MD trajectory. The next two sections outline the techniques used to determine these parameters.

1. The potential of mean force depth $\Delta\phi$

The kinetic decay rate given by Eq. (8) is dominated by the exponential term. Therefore it is imperative that $\Delta\phi$ be well determined.

The mean force is equal to the negative derivative of the potential of mean force $\phi(r)$. It is expressed through a integral relation along the radius r, from the cluster's center of mass position 0, as shown in Eq. (9),

$$\phi(r) = -\int_0^r f(R)dR. \tag{9}$$

The mean force is calculated by evaluating the component of the total force on a molecule acting toward the cluster's center of mass position. This is calculated for every molecule in the cluster for all cluster configurations. The mean radial force for a set of closely spaced radii covering the range of motion is calculated, and is numerically integrated using Eq. (9). Figure 2 is an example of the potential of mean force obtained in this way from a MD simulation of a 67-molecule cluster at 300 K, which shows the depth of the potential of mean force to be about $12kT$.

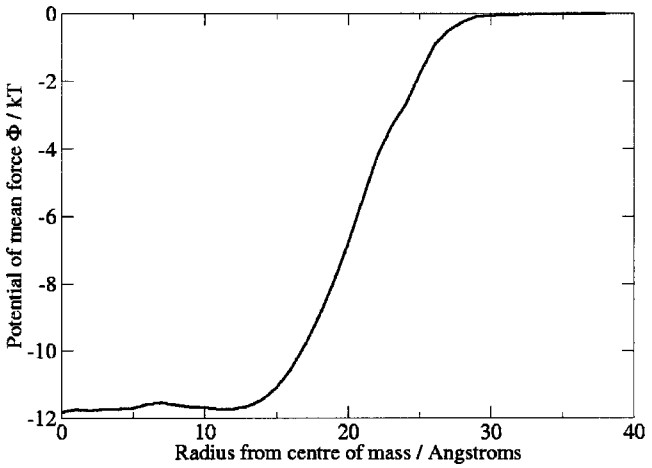

FIG. 2. The potential of mean force for a 67-molecule *n*-nonane cluster simulated at a temperature of 300 K for approximately 5 ns. Clearly the force sampling at the cluster's center of mass is rather noisy as we might expect. For this MD trajectory a decay event was observed half way through the simulation (see Fig. 1).

This method of calculating the potential of mean force relies on good averaging. However, since in the periphery of the cluster the mean particle density is lower than in the cluster body, the accuracy of the averaging for these peripheral regions will be poorer, which means the potential of mean force may not be well characterized. This is most apparent in the absence of decay, and for the *n*-nonane clusters at the temperatures considered, we expect to see few or no decay events during a 5 ns simulation, which could leave the mean force undefined for the cluster's outer regions. However, we must obtain a complete description of the potential mean force for all cluster radii in order to determine the depth $\Delta\phi$.

In the absence of cluster decay we introduce a far field construction to describe the potential of mean force, approximately, for the outer regions. The far field construction method assumes an equivalence between the mean force beyond the cluster's escape radius r_e and the radial derivative of the mean potential energy of a molecule placed at that location. As the radial distance between the cluster and an escaped molecule becomes large, the difference between the potential of mean force and the mean molecule-cluster potential energy is small. Although the two quantities are fundamentally different they converge as $r \to \infty$. This is because when the interaction between the molecule and cluster is weak, the difference between these two quantities becomes insensitive to the differences between molecular configurations of the cluster.

The construction method quantitatively describes the variation of the potential of mean force in the far field, which makes a significant contribution to the depth. We do this by evaluating the mean potential energy $\langle U(r)\rangle$ of an imaginary decay molecule at a radial position r outside the cluster, integrating over a random set of orientations. The derivative of the mean molecule-cluster potential energy and the previ-

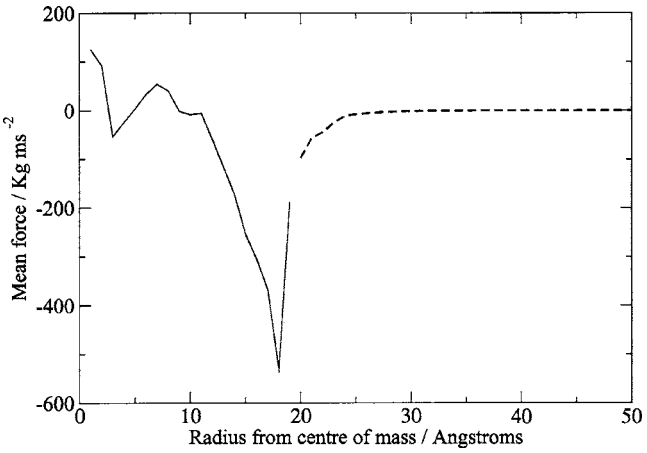

FIG. 3. The far field construction (dashed line) and the mean force within the cluster radius (black solid line). The data shown is obtained from a 40 -molecule cluster at 225 K.

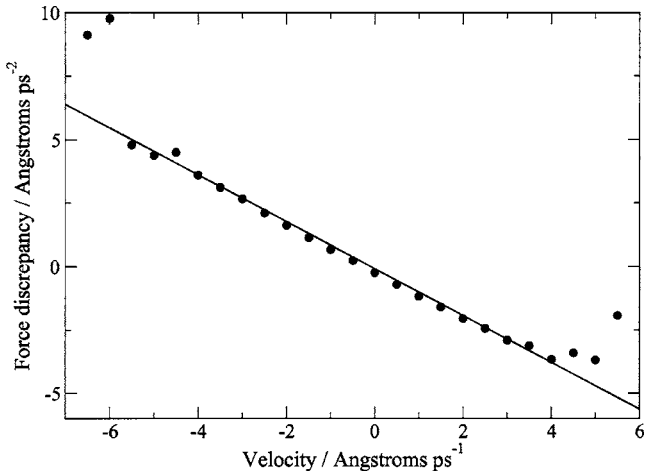

FIG. 4. The average force discrepancy per unit mass acting on a cluster molecule (the 40 cluster) over the coarse grained time interval $\delta t=0.1$ ps plotted against the velocity of a single molecule. The plot illustrates the linear correlation between the discrepancy force and velocity, and the dashed line shows the fit to the expected linear behavior. The gradient of the dashed line is the negative of the friction coefficient γ. The zero intercept suggests that the stochastic force has a zero mean, which is an expected result.

ously derived potential of mean force $\phi(r)$, are shown in Fig. 3 against radius, for a 40 molecule cluster at 225 K.

Although the two curves have a consistent shape, and a similar gradient at r_e, clearly there is a small quantitative disparity between the two values. This could be because cluster molecules are used as conformational templates for the imaginary decay molecules instead of real decay conformations. Since a molecule inside the cluster is interacting strongly with the other molecules, this will affect its conformation, whereas a decay molecule that has escaped from the cluster is not surrounded by the same molecules, and is likely to have a different conformation. Another possibility may be due to a poorly equilibrated cluster configurations, since the potential energy is conformation-averaged but not time-averaged, which could result in an inaccurate potential-energy value. The quantitative difference between the mean potential energy and potential of mean force is small enough to be resolved by interpolation between the two curves. This combines the actual force acting on molecules inside the cluster (determined by MD) with the force predicted to act on a molecule outside the cluster, determined by the far field construction. The total force is numerically integrated from radius 0 to ∞ to give an estimate of the complete potential of mean force for all radii, including in the cluster's periphery.

Since the construction method allows us to identify the magnitude of potential of mean force variation beyond r_e, we can expect it to give a good estimate of the well depth $\Delta\phi$.

2. The friction coefficient γ

The kinetic decay rate in Eq. (8) is inversely proportional to the friction coefficient γ. Typically, frictional forces occur when a particle moves through a static fluid, and to a first approximation the opposing force it experiences is proportional to its velocity. The friction coefficient defines the time scale over which the particle's velocity loses memory of its previous history.

To obtain the friction coefficient for *n*-nonane cluster molecules, we explicitly map the deterministic molecular dynamics of the simulations onto the stochastic dynamics of the Langevin equation. Essentially we resolve the dynamics over a coarse-grained time scale in an attempt to observe the friction force. The Langevin equation for a noise-driven dissipative system is recast as shown in Eq. (10),

$$\gamma m\dot{r} = \langle f(r) - m\ddot{r}\rangle + \langle\tilde{f}\rangle. \tag{10}$$

The brackets refer to a time averaging over a coarse time scale δt. $\langle f(r)\rangle$ reduces simply to $f(r)$ since it is the mean force at radial position r, and we have already determined it from the MD simulations. The final term on the right-hand side is zero by definition. Recast in this form, Eq. (10) connects the frictional force to a radial discrepancy force defined as the difference between the mean radial force and the apparent radial component of the inertial force suggested from the MD over a coarse-grained time scale. We estimate $m\ddot{r}$ from the backward velocity difference at time t, evaluated over varying coarse-grained time intervals δt for a given molecule in the cluster,

$$m\ddot{r} = m\frac{v(t) - v(t-\delta t)}{\delta t}. \tag{11}$$

In the limiting case where the coarse-grained time interval is equal to the MD time step, the force discrepancy should be equal to zero, which means that there are no friction contributions.

The coarse-grained time interval is an arbitrary value, and we choose it to be larger than the MD time scale to avoid sampling deterministic forces, but smaller than the time taken for a molecule to lose its memory to avoid stochastic forces. We begin with the value of $\delta t=0.1$ ps, and plot the radial force discrepancy against radial velocity relative to the cluster's center of mass motion, which is shown in Fig. 4.

The calculation is repeated by increasing δt by a finite value, of 0.025 ps, which gives a range of coarse-grained time intervals that yield similar correlations between discrepancy force and velocity, as shown in Fig. 5. Clearly we can

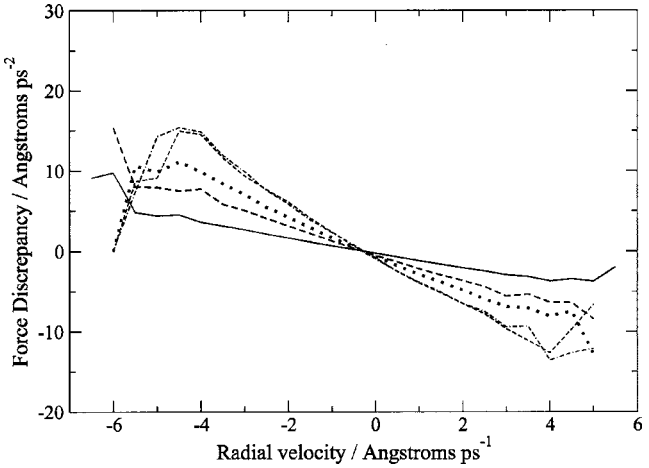

FIG. 5. The radial components of the force discrepancy against velocity evaluated for six different coarse-grained time intervals. Solid line: 0.025 ps; long-dashed line: 0.05 ps; dotted line: 0.075 ps; short-dashed line: 0.15 ps; and dotted dashed line: 0.2 ps.

see that the gradient, which we interpret to be the friction coefficient increases steadily with δt until it reaches an unchanging value. We plot the variation in gradient against the coarse-grained time interval to observe the behavior of the friction coefficient, as shown in Fig. 6.

The curve shows that the friction coefficient is small for time scales of about δt 0.025 ps, but then increases with δt reaching a plateau at 3.0 ps^{-1}. γ is measured to be this value, and the reciprocal of 3.0 ps^{-1} should give a general indication of the time scale over which friction forces act in the system. Indeed, this is reasonably self-consistent with the coarse-grained time scale δt at which γ reaches a plateau.

This value of γ defines the time scale beyond which MD can be mapped onto Langevin dynamics. For very short time scales ($\delta t < 0.025$ ps) deterministic forces dictate the system's dynamics, and each molecule will follow a time-reversible trajectory. For $\delta t > 0.15$ ps the linear correlation between the force discrepancy and velocity becomes difficult to resolve amidst the noise, and a Langevin interpretation of the dynamics is no longer appropriate.

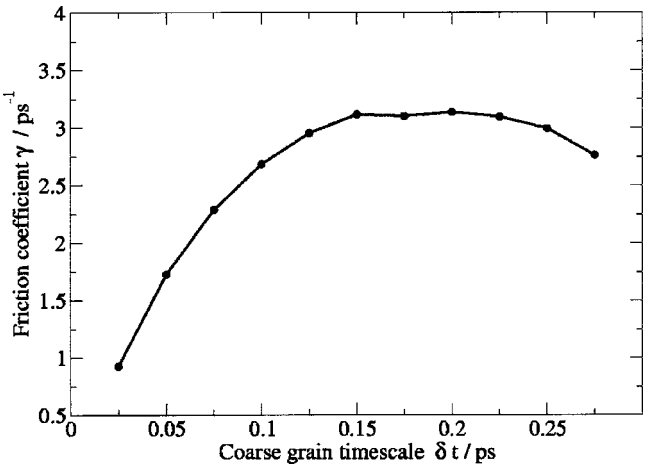

FIG. 6. The friction coefficient for varying coarse-grained time scales δt, calculated from a 40-molecule cluster trajectory at 225 K shows that the apparent γ reaches a plateau at about 3 ps^{-1}. Therefore we expect the friction time scale to be the inverse of this value, and indeed δt does appear consistent with this.

TABLE I. The simulated cluster sizes at their corresponding temperatures with empirical decay times τ_{emp}, dynamically generated decay times τ_{kin} (with estimated errors), and classically derived decay times τ_{class}. For the 40- and 50-sized clusters, the dynamically generated kinetic decay times are reasonably consistent with the empirical decay times. For these clusters sizes the classical decay times compare very poorly to the empirical decay times, and for the smallest cluster size this difference is almost as large as two orders of magnitude.

Cluster Size i	Temperature (K)	τ_{emg} (ns)	τ_{kin} (ns)	τ_{CNT} (ns)
40	225	47	74^{+49}_{-30}	3095
50	250	7	$4.6^{+3.2}_{-1.8}$	178
67	300	0.5	44^{+29}_{-17}	3.2

IV. RESULTS AND DISCUSSION

The kinetic decay model presented in this paper is part of a continuing piece of research. It has been extended in this study to describe a more complex cluster dynamic, which includes molecular bond vibrations, rotations, and torsions. We use the kinetic decay model to calculate mean kinetic decay times for *n*-nonane cluster sizes of 40, 50, and 67 molecules, using Eq. (7). The error in determining $\Delta\phi$ is estimated from the potential of mean force plot (Fig. 2 to be approximately $\pm 0.5kT$). The same plot is used to estimate the error on the cluster radius r_e, which is about ± 2 Å. The error in determining γ is estimated from Fig. 6 to be ± 0.1 ps^{-1} but this will be less significant than the error on $\Delta\phi$ since γ does not appear in the exponent.

We also calculate the classical decay time which is determined from the widely used but inaccurate approximation of CNT applied to molecular clusters. We expect the classical decay time to be a poor estimate of real decay times, and aim to do better through our kinetic decay model. We make quantitative comparisons of these two methods against empirical estimates, which are shown in Table I.

Overall, it appears that the interaction model taken to represent the cluster behavior, together with the Langevin interpretation of the dynamics, provides a reasonably successful description of the real cluster behavior.

The results show that our dynamically generated kinetic decay times make good comparisons to the empirical decay times, which is a significant improvement to the classical estimates. The disagreement between the classical and empirical decay times is most apparent for the 40- and 50-sized clusters. This is where we might expect the CNT treatment of molecular clusters to breakdown, precisely for the smaller cluster sizes.

In contrast, the kinetic decay time for the largest cluster size compares worse to the empirical time scales than that suggested by CNT. This may be due to insufficient data from the MD simulations, which could lead to an incorrect characterization of the potential of mean force for the 67 cluster size. The MD simulations are computationally demanding calculations, even for the smaller cluster sizes. This may be partly due to the imposing thermostat, and we seek to improve this algorithm to eliminate this computational constraint, since it imposes an important factor on larger cluster sizes.

These issues comprise the future prospects of this work, and need to be investigated further in order to characterize this apparent classical breakdown, and to identify the exactly when CNT becomes an unsuitable means of calculating decay times of molecular clusters. This is an important characterization to make because the signature breakdown of CNT for small cluster sizes forces the emphasis of cluster decay studies solely upon the kinetic decay model. This is an important implication not only for small clusters but for clusters with long decay time scales, since decay times cannot be measured from direct observations of simulations. Hence, there remains an ongoing need to establish a reliable method that combines theory and computation to correctly deduce the lifetime of small molecular clusters that maintain a longevity.

V. CONCLUSIONS

The dynamical route by which a molecular cluster reaches a critical size is a complex and uncertain process brought about by a series of fortunate events: the gain and retention of molecules against a tendency for them to be lost. This investigation has developed dynamical insight into the stability of clusters of *n*-nonane using a combination of molecular and Langevin dynamics. We wish to provide the key to a better theoretical understanding of the evaporation processes of quasibound molecular clusters.

The cluster decay model uses dynamically generated forces to parametrize a Langevin equation, which is then used to determine the kinetic evaporation rate of molecular clusters. The Langevin parameters, $\Delta\phi$ and γ, obtained from the MD simulations are characterized by the molecule's center of mass motion, and hence correspond to an average over all the internal degrees of freedom. The simulations mimic the experimental conditions under which the clusters were deduced to be critical. We treat the evaporation of a molecule from a cluster as a single-particle escape from a potential of mean force, driven by its interactions with all the surrounding molecules in the cluster. The mean interactions characterize the shape of the potential of mean force, and, in particular, the well depth $\Delta\phi$.

In the absence of cluster decay, the mean force on molecules occupying regions just beyond the cluster's periphery are not completely sampled. Consequently the potential of mean force for this region is not well established and the potential well depth cannot be correctly quantified. In order to address this shortcoming, the mean force in these regions is approximated by the radial derivative of the mean potential energy of an artificial molecule placed there. Fundamentally the mean potential energy describes the energy needed to remove a particle from a position r within the cluster to ∞. The potential of mean force is not the same as the mean potential energy, but in the limit of large r these two quantities are equivalent.

The friction force is characterized by the coefficient γ, which is extracted from an analysis involving the mapping of the molecular dynamics onto coarse time scale Langevin dynamics. The difference between the force on a molecule evaluated over a coarse time scale, and the MD force on a molecule, averaged over all molecular configurations, is referred to as the mean discrepancy force. We find that it has a linear correlation with the molecule's velocity, with a slope that is related to the friction coefficient γ. We expect γ to rise to a plateau as a function of time scale, and use this value of γ as our estimate.

The cluster decay model is an essential tool for systems with long decay time scales, for which decay events may not be observed during a typical MD trajectory. Overall, it appears that the interaction model taken to represent the cluster behavior, together with the Langevin interpretation of the dynamics, provides a successful description of the real cluster behavior, particularly for the 40 and 50 cluster sizes. This a significant improvement to the decay times suggested by classical nucleation theory for these smallest cluster sizes. However, for the largest cluster size there appears to be a closer correlation with CNT. Further simulations of varying cluster sizes would help characterize the decay model so that it can be applied to a complete distribution of cluster sizes.

Overall, this kinetic treatment of cluster decay provides a fresh approach to modeling a complex microscopic process, and may be used to help develop new theoretical approaches to predict the rate of nucleation. However, there still remains uncertainties particularly concerned with the limitations of simulating complex, long-lived clusters. This reinforces the need to pursue an appropriate and reliable formalism that correctly characterizes the stability of clusters that contain very few molecules.

ACKNOWLEDGMENTS

This research was supported by the UK Natural Environment Research Council under Grant No. NER/T/S/2000/01029. The authors are also grateful for the help and support of PhD student Sascha Khakshouri.

[1] M. Volmer and A. Weber, Z. Phys. Chem., Stoechiom. Verwandtschaftsl. **119**, 277 (1926).
[2] R. Becker and W. Döring, Ann. Phys. **24**, 719 (1935).
[3] D. Kashchiev, *Nucleation: Basic Theory with Applications* (Butterworth Heinemann, Washington, D.C., 2000).
[4] H. C. Hung, M. J. Krasnopoler, and J. L. Katz, J. Chem. Phys. **90**, 1856 (1988).
[5] I. J. Ford, J. Chem. Phys. **105**, 8324 (1996).
[6] D. W. Oxtoby and D. Kashchiev, J. Chem. Phys. **100**, 7665 (1994).
[7] I. J. Ford, Phys. Rev. E **56**, 5615 (1997).
[8] N. Bohr, *The Collected Works* (North-Holland, Amsterdam, 1985), Vol. 6, p. 316.
[9] J. Uffink and J. L. van Dis, Found. Phys. **29**, 655 (1999).
[10] S. A. Harris and I. J. Ford, J. Chem. Phys. **118**, 9216 (2003).
[11] H. C. Anderson, J. Chem. Phys. **72**, 2384 (1979).
[12] I. J. Ford and S. A. Harris, J. Chem. Phys. **120**, 4428 (2004).
[13] X. Daura, A. E. Mark, and W. F. van Gunsteren, J. Chem. Phys. **19**, 535 (1997).
[14] L. D. Schuler, X. Daura, and W. F. van Gunsteren, J. Chem. Phys. **22**, 1205 (2001).
[15] S. Lifson, A. T. Hagler, and P. Dauber, J. Am. Chem. Soc. **101**, 5111 (1979).
[16] A. R. Leach, *Molecular Modelling: Principles and Applications*, 2nd ed. (Prentice-Hall, Englewood Cliffs, New Jersey, 2001).